

SAM-UNet: Enhancing Zero-Shot Segmentation of SAM for Universal Medical Images

Sihan Yang¹, Haixia Bi^{2*}, Hai Zhang³, Jian Sun⁴

¹School of Software Engineering, Xi'an Jiaotong University, Xi'an, China

²School of Information and Communications Engineering, Xi'an Jiaotong University, Xi'an, China

³School of Mathematics, Northwest University, Xi'an, China

⁴School of Mathematics and Statistics, Xi'an Jiaotong University, Xi'an, China

hankyang428@stu.xjtu.edu.cn, haixia.bi@xjtu.edu.cn, zhanghai@nwu.edu.cn, jiansun@xjtu.edu.cn

Abstract

Segment Anything Model (SAM) has demonstrated impressive performance on a wide range of natural image segmentation tasks. However, its performance significantly deteriorates when directly applied to medical domain, due to the remarkable differences between natural images and medical images. Some researchers have attempted to train SAM on large scale medical datasets. However, poor zero-shot performance is observed from the experimental results. In this context, inspired by the superior performance of U-Net-like models in medical image segmentation, we propose SAM-UNet, a new foundation model which incorporates U-Net to the original SAM, to fully leverage the powerful contextual modeling ability of convolutions. To be specific, we parallel a convolutional branch in the image encoder, which is trained independently with the vision Transformer branch frozen. Additionally, we employ multi-scale fusion in the mask decoder, to facilitate accurate segmentation of objects with different scales. We train SAM-UNet on SA-Med2D-16M, the largest 2-dimensional medical image segmentation dataset to date, yielding a universal pretrained model for medical images. Extensive experiments are conducted to evaluate the performance of the model, and state-of-the-art result is achieved, with a dice similarity coefficient score of 0.883 on SA-Med2D-16M dataset. Specifically, in zero-shot segmentation experiments, our model not only significantly outperforms previous large medical SAM models across all modalities, but also substantially mitigates the performance degradation seen on unseen modalities. It should be highlighted that SAM-UNet is an efficient and extensible foundation model, which can be further fine-tuned for other downstream tasks in medical community. The code is available at <https://github.com/Hhankyangg/sam-unet>.

1 Introduction

Segmentation is a fundamental task in medical image analysis, which aims to identify regions of interest (ROIs), such as organs, lesions and tissues, in various medical images. Accurate medical image segmentation is critical for clinical applications such as disease diagnosis, treatment planning and monitoring of disease progression (De Fauw et al. 2018). With the widespread application of deep learning, many segmentation tasks have been automated or semi-automated via models like U-Net (Ronneberger, Fischer, and Brox 2015)

*Corresponding author.

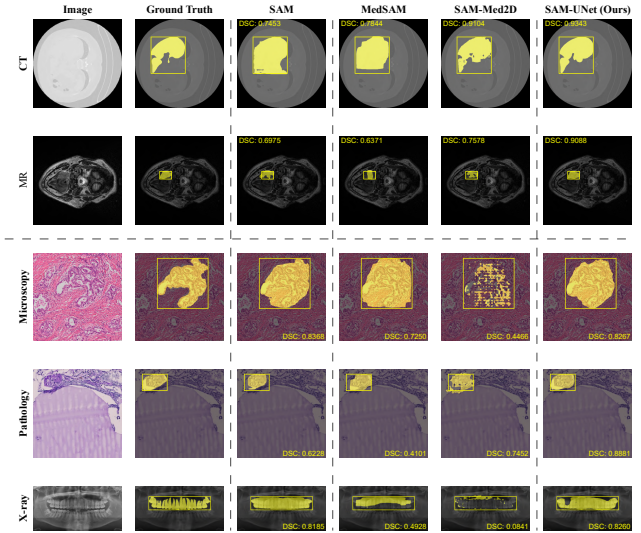


Figure 1: Comparison of our proposed SAM-UNet-50 against existing SAM-based models in terms of zero-shot segmentation performance on modalities with massive samples in the training set: CT & MR, as well as on modalities with limited or no samples in the training set: Microscopy, Pathology & X-ray.

and nnU-Net (Isensee et al. 2021). However, the diversity of segmentation targets has triggered the trend to develop specialized segmentation tools, most of which are customized for specific modalities or disease. These tools often encounter significant performance degradation when applied to other tasks, hampering their generalizability and adaptability, and posing a major obstacle to their broader application in clinical practice.

Most recently, Segment Anything Model (SAM) (Kirillov et al. 2023) has emerged as a powerful large foundational model for natural image segmentation, which is trained on a large-scale natural image dataset (SA-1B). It allows users to generate masks for specific ROIs through interactive clicks, bounding boxes or natural language prompts, which has demonstrated exceptional zero-shot segmentation performance across various vision tasks. This advancement has also propelled the evolution of medical image segmenta-

tion. However, due to significant differences between natural and medical images, SAM struggles to achieve satisfactory zero-shot segmentation performance on medical images (He et al. 2023; Mazurowski et al. 2023; Huang et al. 2024).

Some studies (Ma et al. 2024; Cheng et al. 2023b) have endeavored to build large-scale medical image segmentation datasets and fine-tune SAM. Nevertheless, these datasets suffer from poor diversity and severe imbalances on modalities or organs. To be specific, most of these datasets are predominantly composed of images with MR and CT modalities, and their data volume is far smaller compared to SA-1B which contains 1 billion masks. As a result, SAM fine-tuned on these datasets may only outperform the original SAM in certain medical image modalities, while in other less common modalities, its segmentation performance is even inferior to the original SAM, as illustrated in Figure 1. To address the zero-shot performance degradation issue and further comprehensively enhance SAM’s capabilities in medical image segmentation, we propose SAM-UNet, a novel SAM-based foundation model designed from the architectural level, which is inspired by the huge success of U-Net and other U-shaped networks in image segmentation.

Specifically, we introduce two architectural designs in the image encoder and mask decoder respectively. First, we incorporate a parallel convolutional neural network (CNN) branch in the image encoder, with the original Vision Transformer (ViT) branch completely frozen to preserve SAM’s natural image encoding capabilities. The inclusion of convolutions is attributed to their superior feature extraction abilities on smaller datasets (Raghu et al. 2021) and their outstanding capacity in local information modeling. Additionally, the integration of CNN with ViT (Ji et al. 2021; Zhang, Liu, and Hu 2021) has consistently produced new state-of-the-art (SOTA) results. In the mask decoder, inspired by U-Net, we leverage a multi-scale fusion strategy to enable accurate segmentation of multi-scale objects. We further adopt an output token design (Ke et al. 2024), making the mask decoder more specialized for the medical domain.

Two versions of SAM-UNet, namely SAM-UNet-34 and SAM-UNet-50, are trained on the largest medical segmentation dataset to date, SA-Med2D-16M (Ye et al. 2023). Experiments show that SAM-UNet achieves state-of-the-art segmentation performance on all modalities in the test set.

Notably, we conducted extensive zero-shot segmentation experiments on seven medical image datasets which are unseen in the training set and compared them with existing models. Results suggest that in modalities with a wealth of samples in training set, such as CT and MR, SAM-UNet yields the best performance, and in modalities with fewer or no samples, such as Microscopy, Pathology and X-ray, SAM-UNet exhibits comparable performance compared with SAM. Figure 1 presents some visual examples of these zero-shot experiments.

In summary, the contributions of this paper are threefold:

- We introduce architectural innovations, including the integration of a parallel CNN branch in the image encoder and the multi-scale fusion design in the mask decoder, which constitute a new approach for partial parameter

fine-tuning of SAM, both of which have proven effective in improving segmentation performance.

- We propose SAM-UNet, a powerful foundational model trained on SA-Med2D-16M, enhancing zero-shot segmentation capabilities of SAM on universal medical images. SAM-UNet achieves superior performance across diverse medical image modalities (a DSC score of 0.883 on SA-Med2D-16M test set). We develop two versions of SAM-UNet, i.e., SAM-UNet-34 and SAM-UNet-50, where SAM-UNet-50, with a larger parameter scale, demonstrates particularly strong performance.
- We conduct zero-shot segmentation experiments on seven external datasets, demonstrating that SAM-UNet remarkably outperforms existing SAM-based models. SAM-UNet shows exceptional performance in modalities well-represented in the training set, such as CT and MR, and maintains robust performance without significant degradation in less common modalities.

2 Related Work

2.1 CNN and Transformer for Medical Image Segmentation

U-Net (Ronneberger, Fischer, and Brox 2015) was proposed for medical image segmentation and quickly became a mainstream method due to its powerful ability to extract local features by convolutions and its simple yet effective U-shaped encoder-decoder architecture. Its successfully led to the development of various improved versions of U-Net, such as UNet++ (Zhou et al. 2018), ResUNet++ (Jha et al. 2019) and Attention U-Net (Oktay et al. 2018). In recent years, DconnNet (Yang and Farsiu 2023) has become a SOTA CNN-based segmentation model.

Meanwhile, with the advent of ViT (Dosovitskiy et al. 2020), researchers began to introduce Transformers into the field of computer vision and explored its application in medical image segmentation. Among various Transformer-based works, Swin-Unet (Cao et al. 2022) stands out as the first pure Transformer-based U-shaped architecture.

Although Transformers shows evident advantages in capturing global information, their lack of fixed receptive fields makes them less precise at edges. To tackle this issue, researchers have thus combined CNN and Transformers, forming new architectures and training strategies. For example, TransFuse (Zhang, Liu, and Hu 2021) proposed to integrate multi-level feature maps from both Transformer and CNN branches for medical image segmentation, while MC-Trans (Ji et al. 2021) exploited multi-scale convolutional features as token sequences to perform attention computations. Additionally, MedT (Valanarasu et al. 2021) not only introduced gated axial-attention model but also proposed a local-global training strategy for medical image segmentation.

2.2 Segmentation Anything Model

SAM (Kirillov et al. 2023) is a pioneering foundation model for image segmentation, particularly focused on interactive segmentation tasks. Pre-trained on a large-scale image segmentation dataset, SA-1B, SAM is equipped with the excellent zero-shot segmentation capabilities. SAM has also led

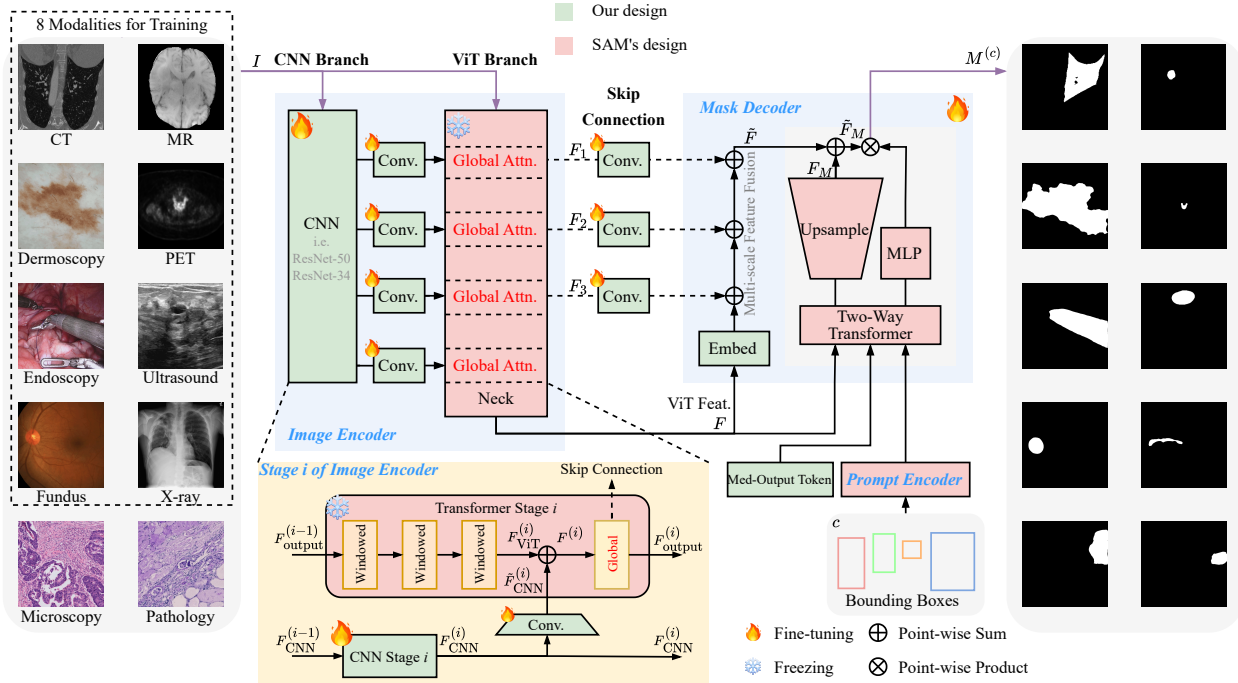


Figure 2: The pipeline of SAM-UNet. The model consists of a two-branch image encoder and a multi-scale fusion mask decoder. It is trained using bounding boxes as prompts on a large dataset containing the eight modalities shown in the figure and tested on all ten modalities. The figure also illustrates the details of each stage in the image encoder.

to numerous follow-up works that aim to optimize SAM’s segmentation performance through fine-tuning or model architecture modifications.

Fine-tuning Both full fine-tuning and parameter-efficient fine-tuning have been conducted on SAM on specific downstream tasks. For instance, MedSAM (Ma et al. 2024) full fine-tuned SAM on medical images across multiple modalities and anatomical regions, while SAMed (Zhang and Liu 2023) leveraged Low-Rank Adaptation (LoRA) (Hu et al. 2021) to enhance the performance with minimal parameter adjustments on targeted downstream tasks.

Model Architecture Modifications Several studies have also focused on altering the original structure of SAM to achieve better segmentation performance. These modifications generally target either the image encoder or the mask decoder. For example, SAMUS (Lin et al. 2023) introduced a parallel CNN branch to the image encoder, facilitating information exchange between branches via cross-attention, while H-SAM (Cheng et al. 2024) divided the decoding process into two stages, where the decoder in the first stage generates a prior probabilistic mask that guides a more intricate decoding in the second stage.

2.3 Foundation Model for Medical Image Segmentation

Large-scale models pre-trained on vast datasets have significantly propelled the advancement of deep learning. These models often possess strong zero-shot learning capabilities

and serve as robust initial models for transfer learning. However, research on foundation models for medical image segmentation remains relatively scarce. Before the emergence of SAM, Huang et al. proposed a large-scale model (up to 1.4 billion parameters), STU-Net (Huang et al. 2023), trained on a dataset comprising multiple categories of medical images. Similarly, UniverSeg (Butoi et al. 2023) introduced a new paradigm for medical image segmentation, enabling segmentation of universal medical images in a manner akin to few-shot learning.

Following SAM, researchers discovered new pathways for leveraging large vision models (LVM) in medical image analysis, where MedSAM and SAM-Med2D are forerunners on this way (Cheng et al. 2023b). MedSAM was fully fine-tuned on a dataset containing approximately 1.5 million image-mask pairs, while SAM-Med2D employed adapter tuning techniques to fine-tune SAM on SA-Med2D-20M (Ye et al. 2023) dataset.

3 Method

3.1 Preliminaries

Before delving into the details of SAM-UNet, it is essential to briefly review the architecture of SAM.

SAM is composed of three components: a large-scale image encoder, a prompt encoder and a lightweight mask decoder. The image encoder exploits a ViT (Li et al. 2022) to process high-resolution images and generate feature maps at 1/16 scale of the original image. The prompt encoder accepts

both sparse and dense prompts, including points, bounding boxes or masks, converting them into 256-dimensional vectors. The mask decoder then employs a lightweight cross-attention mechanism to integrate the embeddings from the image and prompt encoders, allowing SAM to generate different masks for the same image based on diverse prompts.

3.2 Overview

In this work, we introduce SAM-UNet, a novel foundation model that enhances SAM by integrating a U-Net-like architecture to improve its performance on medical image segmentation tasks. Specifically, given a pre-processed medical image $I \in \mathbb{R}^{3 \times H \times W}$ with a bounding box prompt c specifying the target region, our goal is to predict the corresponding binary mask $M^{(c)}$:

$$M^{(c)} = \text{SAM-UNet}(I, c) \quad (1)$$

As shown in Figure 2, SAM-UNet incorporates a parallel CNN branch in the image encoder, which is trained independently while the ViT branch remains frozen, to preserve the generalization capabilities of the ViT while enhancing the model’s ability to capture fine-grained features in medical images. We also introduce multi-scale fusion within the mask decoder to further promote the segmentation accuracy. Based on different CNN branches, two versions of SAM-UNet are released: SAM-UNet-34 and SAM-UNet-50, which correspond to the use of ResNet-34 (He et al. 2016) and ResNet-50, respectively. SAM-UNet is trained on SA-Med2D-16M, the largest 2D medical image segmentation dataset available, focusing exclusively on bounding box prompts, as they are widely recognized by researchers to perform best on medical images (Cheng et al. 2023b; Huang et al. 2024; Cheng et al. 2023a; Zhang, Shen, and Jiao 2024).

In the following sections, we will discuss the components of SAM-UNet and the training process in detail.

3.3 Two-Branch Image Encoder

In ViT-B SAM, even with the smallest parameter scale, the image encoder contains approximately 86M parameters, making full parameter fine-tuning computationally challenging. On the other hand, directly fine-tuning the ViT encoder on small-scale dataset would result in obvious degradation on the model’s zero-shot segmentation performance. To address this dilemma, we propose a two-branch image encoder architecture that incorporates a CNN branch to the original ViT branch. Under this design, only the CNN branch, which has remarkably fewer parameters, is trained during training stage, with the ViT branch frozen.

It is important to note that the image encoder in all versions of SAM consists of four stages, each comprising several window attention Transformer blocks and one global attention Transformer block. To optimize memory usage and accelerate the inference process, SAM-UNet uses the ViT-B version of SAM as the initial model. To match the four-stage design of ViT, the integrated parallel CNN is composed of four stages as well. Concretely, we adopt ResNet-34 and ResNet-50 as the backbone networks of the CNN branch.

First, the pre-processed RGB medical image is fed into both the ViT and CNN branches (see steps 1-3 in Algorithm

1). At each subsequent stage, the ViT branch processes the output feature map from the previous stage $F_{\text{output}}^{(i-1)}$ through window attention blocks $\text{ViT}_{\text{window}}^{(i)}$, generating a new feature map $F_{\text{ViT}}^{(i)}$. Simultaneously, the CNN branch uses its respective convolutional layers $\text{CNN}^{(i)}$ to generate a new feature map $F_{\text{CNN}}^{(i)}$, which is then convolved via $\text{Conv}^{(i)}$ to match the shape of the ViT feature map $\tilde{F}_{\text{CNN}}^{(i)}$. At each stage, the transformed CNN feature map is point-wise added to the ViT feature map, resulting in a fused feature map $F^{(i)}$. This map is next processed by the global attention block $\text{ViT}_{\text{global}}^{(i)}$, producing the output feature map for the current stage $F_{\text{output}}^{(i)}$ (see steps 5-10 in Algorithm 1). This process is repeated across all four stages. After the fourth stage, the final output feature map $F_{\text{output}}^{(4)}$ is further processed by the ViT neck layer ViT^{neck} , generating the final encoded feature map F (see steps 4-12 in Algorithm 1).

Algorithm 1: Two-Branch Image Encoder in SAM-UNet

Input: Pre-processed medical image $I \in \mathbb{R}^{3 \times H \times W}$

Output: Feature map after image encoder $F \in \mathbb{R}^{256 \times \frac{H}{16} \times \frac{W}{16}}$

- 1: Initialize:
 - 2: Compute $F_{\text{output}}^{(0)} = \text{PatchEmbed}(I)$
 - 3: Compute $F_{\text{CNN}}^{(0)} = \text{CNN}^{(0)}(I)$
 - 4: **for** $i = 1$ **to** 4 **do**
 - 5: **ViT Branch:** Compute $F_{\text{ViT}}^{(i)} = \text{ViT}_{\text{window}}^{(i)}(F_{\text{output}}^{(i-1)})$
 - 6: **CNN Branch:**
 - 7: Compute $F_{\text{CNN}}^{(i)} = \text{CNN}^{(i)}(F_{\text{CNN}}^{(i-1)})$
 - 8: Compute $\tilde{F}_{\text{CNN}}^{(i)} = \text{Conv}^{(i)}(F_{\text{CNN}}^{(i)})$
 - 9: Point-wise addition: $F^{(i)} = F_{\text{ViT}}^{(i)} + \tilde{F}_{\text{CNN}}^{(i)}$
 - 10: Compute $F_{\text{output}}^{(i)} = \text{ViT}_{\text{global}}^{(i)}(F^{(i)})$
 - 11: **end for**
 - 12: Compute $F = \text{ViT}^{\text{neck}}(F_{\text{output}}^{(4)})$
 - 13: **return** F
-

3.4 Prompt Encoder

Numerous studies (Cheng et al. 2023b; Huang et al. 2024; Cheng et al. 2023a; Zhang, Shen, and Jiao 2024) have demonstrated that in the application of medical image segmentation, bounding boxes provide considerably better segmentation results compared to other types of prompts such as points. Additionally, in practical interactive segmentation tasks, using bounding boxes to signify the approximate segmentation area is not only intuitive but also practical (Ma et al. 2024). Therefore, our work focuses solely on segmentation with bounding boxes as prompts, and our training is conducted exclusively with this type of prompt.

The prompt encoder in SAM-UNet remains consistent with SAM. For each bounding box, the prompt encoder encodes the central positions of the “top-left” and “bottom-right” pixels using positional encoding, producing two 256-dimensional vectors.

3.5 Mask Decoder with Multi-scale Feature Fusion

Two primary modifications are made to the architecture of SAM’s mask decoder, as shown in Figure 3.

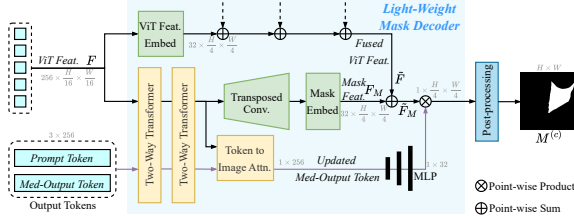


Figure 3: The architecture of our modified mask decoder, featuring a Med-Output Token and a U-Net-like multi-scale fusion branch.

1. **Med-Output Token.** Inspired by SAM-HQ (Ke et al. 2024), we introduce the Med-Output Token (size of 1×256) and discard the IoU prediction token and multiple mask tokens which are used in the original SAM. The reason for SAM adopting the IoU prediction token and multiple mask tokens is that point-based prompts might generate ambiguities in natural images. Therefore, it is reasonable to produce multiple masks and select the most appropriate one based on the IoU prediction score. However, in medical image segmentation scenario with bounding boxes as prompts, such ambiguities are rare, making it unnecessary to output predicted IoU scores and multiple masks. Our ablation studies also demonstrate the effectiveness of this change.

2. **Multi-scale Fusion Branch.** We add a U-Net-like multi-scale fusion branch to the encoder feature map F . Ghiasi et al. show that, similar to CNNs, ViTs retain more edge information in the early Transformer blocks, which can enhance segmentation accuracy—this is also the reason why U-Net-like networks are so effective in segmentation tasks. Therefore, we apply skip connections to the output feature maps F_i from the first three stages of the ViT. They are fused with the dimensionally adjusted F via convolutional layers, resulting in multi-scale fused feature map $\tilde{F} \in \mathbb{R}^{32 \times \frac{H}{4} \times \frac{W}{4}}$. \tilde{F} is then point-wise added to the mask feature F_M , which is obtained by first passing it through two-way Transformer blocks to incorporate information from the output tokens (including prompt tokens and the Med-Output Token) and then up-sampling to $\frac{H}{4} \times \frac{W}{4}$. This operation yields the multi-scale fused feature map \tilde{F}_M .

The updated Med-Output Token, which has acquired global image context and prompt tokens information, is processed through a three-layer MLP, reducing its size to 1×32 . This token is then used in a point-wise product operation with \tilde{F}_M , producing a mask of size $1 \times \frac{H}{4} \times \frac{W}{4}$. After interpolation, padding and other post-processing steps, the mask decoder successfully generates mask $M^{(c)}$ based on the prompt c .

3.6 Training of SAM-UNet

Training Dataset Our training dataset is SA-Med2D-16M (Ye et al. 2023), the largest benchmark dataset for medical image segmentation. It contains medical images from eight different modalities, spanning over 200 categories, with a total of 3.6 million images and 15.8 million masks. The numbers of images across the eight modalities are shown in Table 1. As depicted, CT and MR modalities dominate the dataset. We use a random seed of 0 to split the data for each modality, with 80% used as the training set and the remaining 20% as the test set. All images are first padded to square shapes and then resized to 256×256 before fed into the model.

Modality	CT	Endoscopy	PET	Fundus
Images	1,645,894	4,290	5,410	1,445
Modality	MR	Dermoscopy	X-ray	Ultrasound
Images	1,967,254	6,698	5,581	2,590

Table 1: The number of images of each modality in SA-Med2D-16M.

Loss Function We make the following modifications to the loss function used in (Kirillov et al. 2023) :

1. Since we removed the IoU prediction head from the mask decoder, we no longer compute the mean-square-error loss between the IoU prediction and the predicted mask’s IoU with the ground truth mask.

2. In our experiments, we observe that the dice loss \mathcal{L}_{Dice} is often several times larger than the focal loss \mathcal{L}_{Focal} . To balance these two losses, we adjust their ratio in the original SAM loss function from 1:20 to 20:1.

The final loss function is:

$$\mathcal{L} = 20 \times \mathcal{L}_{Dice} + \mathcal{L}_{Focal} \quad (2)$$

SAM-UNet Training In line with previous studies (Kirillov et al. 2023; Ma et al. 2024; Cheng et al. 2023b), we train SAM-UNet by simulating interactive segmentation. For each image, we randomly select 5 masks associated with the image. For each mask, we generate a bounding box that may deviate from the target region’s bounding box by up to 5 pixels to simulate real-world conditions. During training, we fix the image encoder of the pre-trained SAM model. This results in SAM-UNet-50 which has a total of 138,428,204 parameters, with only 51,755,564 of them being trainable. For SAM-UNet-34, the total number of parameters is 116,019,884, with 29,347,244 trainable parameters. We use a learning rate of 0.0001 and train SAM-UNet for 12 epochs, reducing the learning rate by half after 5 and 10 epochs. Training is conducted on 4 NVIDIA Tesla A100 GPUs, taking approximately 72 hours to complete. In training, each GPU processes 50 images along with their corresponding 250 masks.

4 Experiments

In this section, we conduct three groups of experiments: ablation study, test set comparison experiments, and zero-shot segmentation comparison experiments.

Model	Decoder (trained) with		Image encoder			Test set DSC (%)
	multi-scale fusion	new output tokens	ViT (fixed)	ResNet-34	ResNet-50	
SAM			✓			67.5
SAM-UNet			✓		✓	79.9
					✓	74.0
	✓	✓	✓			74.1
	✓				✓	81.0
		✓	✓		✓	80.9
	✓	✓	✓	✓		80.8
	✓	✓	✓		✓	82.0

Table 2: Ablation study on (1) the two branches in the image encoder, (2) the effects of two adjustments in the decoder, and (3) the impact of different CNN branches. The test set comprises 20% of a randomly selected subset (1/10) from the SA-Med-16M dataset.

Model	PET	X-Ray	Fundus	Ultrasound	CT	MR	Endoscopy	Dermoscopy	Overall DSC
SAM	71.7	55.8	75.7	79.9	72.7	57.2	79.8	86.0	66.6
SAM-Med2D	74.0	60.8	81.8	80.5	80.0	53.0	76.8	91.8	69.4
MedSAM	54.2	50.0	70.4	72.1	59.0	50.9	62.5	84.1	55.8
SAM-UNet-34	90.4	82.5	96.0	92.2	92.4	80.4	90.3	96.8	87.6
SAM-UNet-50	90.9	85.2	97.0	91.0	92.7	81.6	90.8	97.2	88.3

Table 3: Performance comparison of SAM-UNet-50, SAM-UNet-34, SAM-Med2D, MedSAM, and SAM across various modalities on the large-scale test set.

4.1 Experimental Setup

Datasets We use the SA-Med2D-16M dataset for training, as described in Section 3.6. To comprehensively evaluate the zero-shot segmentation performance of SAM-UNet, we conduct experiments on 7 datasets that are not included in the training set: HNTSMRG (Wahid et al. 2024), KiTS23 (Heller et al. 2023), CURVAS (Riera-Marín et al. 2024), STS-2D (Wang et al. 2024), COSAS24 (Liu et al. 2024), KPIs24 (Tang et al. 2024) and EBHI-SEG (MIaMIA 2022).

Data Pre-processing Similar to the approach in (Ye et al. 2023), we first collect all images and masks from the dataset. **(1)** For images, we first normalize the image data. If the image is 3-dimensional, we then slice it to convert all images into 2D RGB format. **(2)** For masks, we first split the semantic masks into binary masks. Next, we separate the binary foreground into multiple connected components. Finally, we remove masks where the target area accounts for less than 0.153% ($\frac{100}{256 \times 256}$) of the whole image area. This process results in multiple binary masks corresponding to each image.

Evaluation Metrics We follow prior researches (Kirillov et al. 2023; Ma et al. 2024; Cheng et al. 2023b) and adopt the Dice Similarity Coefficient (DSC) to evaluate the segmentation results.

4.2 Ablation study

We conduct comprehensive ablation studies on the proposed SAM-UNet, analyzing the impact of each modification made to the original SAM. For the ablation experiments,

due to the large size of the training dataset, we used 1/10 of the SA-Med2D-16M dataset for training and testing. The DSC results of various model variants on the training set are shown in Table 2.

Both Branches in the Image Encoder Are Essential As shown in Table 2, the DSC score of the original SAM is 67.5%, while the addition of the trainable ResNet-50 branch leads to an increase of 12.4% on DSC score. We also attempt to remove the ViT encoder in the original SAM, leaving only the trainable CNN backbone as the image encoder. The result shows that SAM-UNet without the ViT encoder still outperforms the original SAM, but it does not perform as well as SAM-UNet with both branches. These findings demonstrate that both branches are indispensable.

All Adjustments to the Decoder Are Necessary In Table 2, we can observe that merely adjusting the decoder architecture without modifying the image encoder can improve the accuracy of medical image segmentation, but only by 6.5%. Our experiments further demonstrate that, on top of the two-branch image encoder, both the multi-scale feature fusion and the replacement of the original output tokens with the new Med-Output Token can enhance the model’s segmentation performance. Additionally, we can see that the full version of SAM-UNet-50, which incorporates the advantages of all components, achieves the best performance with a DSC score of 82.0%.

ResNet-50 Outperforms ResNet-34 as the CNN Branch In Table 2, the performance of SAM-UNet with ResNet-50

Model	MR		CT		X-ray	Microscopy	Pathology	
	HNTSMRG	KiTS23	CURVAS	STS-2D	COSAS24	KPIs24	EBHI-SEG	
SAM	70.2	89.6	82.1	63.4	66.2	84.8	80.6	
SAM-Med2D	72.2	89.3	90.5	44.2	43.5	70.6	54.1	
MedSAM	62.3	71.2	65.2	59.0	59.7	70.4	77.0	
SAM-UNet-50	85.0	95.3	93.1	73.4	65.1	87.2	79.2	

Table 4: Performance comparison of SAM-UNet-50, SAM-Med2D, MedSAM, and SAM in zero-shot segmentation experiments on unseen modalities and datasets.

as the CNN branch outperforms the version with ResNet-34 by 1.2%. This demonstrates that ResNet-50, with its deeper architecture, provides better feature extraction and contributes to more accurate segmentation results in the SAM-UNet framework.

4.3 Test Set Performance Comparison

Due to the large size of the original dataset, the test set, which was created by randomly selecting 20% of the images from each modality, still includes eight modalities and various categories of masks. We conducted inference on the large-scale test set using our proposed SAM-UNet-34, SAM-UNet-50, and two SOTA SAM-based universal medical image segmentation models, MedSAM (Ma et al. 2024) and SAM-Med2D (Cheng et al. 2023b), along with the original SAM. The segmentation performance for each modality and the overall data is presented in Table 3.

As shown in Table 3, our proposed SAM-UNet-34 and SAM-UNet-50 significantly outperform the other models across all modalities. Notably, compared to SAM-Med2D, which is trained on an extended version of our training dataset, the SAM-UNet architecture is able to learn better domain-specific knowledge for medical image segmentation. Specifically, SAM-UNet-50 achieves the highest DSC scores on most modalities. However, it is noteworthy that for Ultrasound images, SAM-UNet-34, with its simpler convolutional layers, outperforms SAM-UNet-50. This may be due to the fact that Ultrasound images typically have higher noise levels and lower contrast, making the more complex model more prone to overfitting, thereby resulting in lower performance compared to the smaller model.

For SAM and MedSAM, due to differences in the training datasets, the test set segmentation effectively serves as a full zero-shot segmentation task. It is also noteworthy that MedSAM underperforms the original SAM across all modalities. The reason for this is that although MedSAM fine-tunes full parameters of SAM, it is trained on a relatively small dataset with only about 1.5 million image-mask pairs. This limitation not only fails to enhance MedSAM’s zero-shot capabilities but also weakens its ability to encode general image features compared to SAM.

4.4 Zero-Shot Segmentation Performance Comparison

We conduct zero-shot segmentation experiments on seven medical image segmentation datasets which are not included

in our training set, as mentioned in Section 4.1. These experiments are performed using our proposed SAM-UNet-50, MedSAM (Ma et al. 2024), SAM-Med2D (Cheng et al. 2023b) and the original SAM. These seven datasets encompass five different modalities, i.e., CT, MR, X-ray, Pathology and Microscopy, among which the Pathology and Microscopy modalities are not present in our training set. The test results are presented in Table 4.

As for MR and CT modalities which dominate the training datasets, SAM-Med2D achieves slightly better zero-shot segmentation performance than SAM, while MedSAM underperforms SAM—a result we discussed in Section 4.3. Our proposed SAM-UNet-50 model demonstrates superior zero-shot segmentation performance on external datasets for these two modalities.

As shown in Table 1, the X-ray modality data accounts for only 0.2% of the training dataset, while Microscopy and Pathology modalities are not included at all. MedSAM and SAM-Med2D’s datasets share the similar situation, with very few samples from these three modalities. Due to the extremely low representation of these modalities, the strategy of fine-tuning the ViT encoder leads to a significant degradation in zero-shot segmentation performance for MedSAM and SAM-Med2D, falling far behind SAM. However, despite the training dataset being similarly or even more imbalanced, SAM-UNet, benefiting from its fully frozen ViT encoder that retains SAM’s encoding capabilities for natural images and its unique U-shape architecture, manages to maintain comparable performance (around 1% DSC score difference) with SAM on COSAS24 and EBHI-SEG datasets. It even outperforms SAM on STS-2D and KPIs24 datasets.

5 Conclusion

In this paper, we introduce a novel and effective partial parameter fine-tuning architecture for SAM and propose a foundation model, SAM-UNet, trained on the largest available medical image segmentation dataset. Our architectural innovations include a two-branch image encoder and a mask decoder with multi-scale fusion. Our model achieved SOTA performance on the test set and demonstrated more stable and superior performance in zero-shot segmentation across seven external datasets.

References

- Butoi, V. I.; Ortiz, J. J. G.; Ma, T.; Sabuncu, M. R.; Guttag, J.; and Dalca, A. V. 2023. Universeg: Universal medical image segmentation. In *Proceedings of the IEEE/CVF International Conference on Computer Vision*, 21438–21451.
- Cao, H.; Wang, Y.; Chen, J.; Jiang, D.; Zhang, X.; Tian, Q.; and Wang, M. 2022. Swin-unet: Unet-like pure transformer for medical image segmentation. In *European conference on computer vision*, 205–218. Springer.
- Cheng, D.; Qin, Z.; Jiang, Z.; Zhang, S.; Lao, Q.; and Li, K. 2023a. Sam on medical images: A comprehensive study on three prompt modes. *arXiv preprint arXiv:2305.00035*.
- Cheng, J.; Ye, J.; Deng, Z.; Chen, J.; Li, T.; Wang, H.; Su, Y.; Huang, Z.; Chen, J.; Jiang, L.; et al. 2023b. Sam-med2d. *arXiv preprint arXiv:2308.16184*.
- Cheng, Z.; Wei, Q.; Zhu, H.; Wang, Y.; Qu, L.; Shao, W.; and Zhou, Y. 2024. Unleashing the potential of SAM for medical adaptation via hierarchical decoding. In *Proceedings of the IEEE/CVF Conference on Computer Vision and Pattern Recognition*, 3511–3522.
- De Fauw, J.; Ledsam, J. R.; Romera-Paredes, B.; Nikolov, S.; Tomasev, N.; Blackwell, S.; Askham, H.; Glorot, X.; O’Donoghue, B.; Visentin, D.; et al. 2018. Clinically applicable deep learning for diagnosis and referral in retinal disease. *Nature medicine*, 24(9): 1342–1350.
- Dosovitskiy, A.; Beyer, L.; Kolesnikov, A.; Weissenborn, D.; Zhai, X.; Unterthiner, T.; Dehghani, M.; Minderer, M.; Heigold, G.; Gelly, S.; et al. 2020. An image is worth 16x16 words: Transformers for image recognition at scale. *arXiv preprint arXiv:2010.11929*.
- Ghiasi, A.; Kazemi, H.; Borgnia, E.; Reich, S.; Shu, M.; Golub, M.; Wilson, A. G.; and Goldstein, T. 2022. What do vision transformers learn? a visual exploration. *arXiv preprint arXiv:2212.06727*.
- He, K.; Zhang, X.; Ren, S.; and Sun, J. 2016. Deep residual learning for image recognition. In *Proceedings of the IEEE conference on computer vision and pattern recognition*, 770–778.
- He, S.; Bao, R.; Li, J.; Grant, P. E.; and Ou, Y. 2023. Accuracy of segment-anything model (sam) in medical image segmentation tasks. *arXiv preprint arXiv:2304.09324*, 2.
- Heller, N.; Isensee, F.; Trofimova, D.; Tejpaul, R.; Zhao, Z.; Chen, H.; Wang, L.; Golts, A.; Khapun, D.; Shats, D.; Shoshan, Y.; Gilboa-Solomon, F.; George, Y.; Yang, X.; Zhang, J.; Zhang, J.; Xia, Y.; Wu, M.; Liu, Z.; Walczak, E.; McSweeney, S.; Vasdev, R.; Hornung, C.; Solaiman, R.; Schoepfoerster, J.; Abernathy, B.; Wu, D.; Abdulkadir, S.; Byun, B.; Spriggs, J.; Struyk, G.; Austin, A.; Simpson, B.; Hagstrom, M.; Virnig, S.; French, J.; Venkatesh, N.; Chan, S.; Moore, K.; Jacobsen, A.; Austin, S.; Austin, M.; Regmi, S.; Papanikolopoulos, N.; and Weight, C. 2023. The KiTS21 Challenge: Automatic segmentation of kidneys, renal tumors, and renal cysts in corticomedullary-phase CT. *arXiv:2307.01984*.
- Hu, E. J.; Shen, Y.; Wallis, P.; Allen-Zhu, Z.; Li, Y.; Wang, S.; Wang, L.; and Chen, W. 2021. Lora: Low-rank adaptation of large language models. *arXiv preprint arXiv:2106.09685*.
- Huang, Y.; Yang, X.; Liu, L.; Zhou, H.; Chang, A.; Zhou, X.; Chen, R.; Yu, J.; Chen, J.; Chen, C.; et al. 2024. Segment anything model for medical images? *Medical Image Analysis*, 92: 103061.
- Huang, Z.; Wang, H.; Deng, Z.; Ye, J.; Su, Y.; Sun, H.; He, J.; Gu, Y.; Gu, L.; Zhang, S.; et al. 2023. Stu-net: Scalable and transferable medical image segmentation models empowered by large-scale supervised pre-training. *arXiv preprint arXiv:2304.06716*.
- Isensee, F.; Jaeger, P. F.; Kohl, S. A.; Petersen, J.; and Maier-Hein, K. H. 2021. nnU-Net: a self-configuring method for deep learning-based biomedical image segmentation. *Nature methods*, 18(2): 203–211.
- Jha, D.; Smedsrud, P. H.; Riegler, M. A.; Johansen, D.; De Lange, T.; Halvorsen, P.; and Johansen, H. D. 2019. Resunet++: An advanced architecture for medical image segmentation. In *2019 IEEE international symposium on multimedia (ISM)*, 225–2255. IEEE.
- Ji, Y.; Zhang, R.; Wang, H.; Li, Z.; Wu, L.; Zhang, S.; and Luo, P. 2021. Multi-compound transformer for accurate biomedical image segmentation. In *Medical Image Computing and Computer Assisted Intervention—MICCAI 2021: 24th International Conference, Strasbourg, France, September 27–October 1, 2021, Proceedings, Part I 24*, 326–336. Springer.
- Ke, L.; Ye, M.; Danelljan, M.; Tai, Y.-W.; Tang, C.-K.; Yu, F.; et al. 2024. Segment anything in high quality. *Advances in Neural Information Processing Systems*, 36.
- Kirillov, A.; Mintun, E.; Ravi, N.; Mao, H.; Rolland, C.; Gustafson, L.; Xiao, T.; Whitehead, S.; Berg, A. C.; Lo, W.-Y.; et al. 2023. Segment anything. In *Proceedings of the IEEE/CVF International Conference on Computer Vision*, 4015–4026.
- Li, Y.; Mao, H.; Girshick, R.; and He, K. 2022. Exploring plain vision transformer backbones for object detection. In *European conference on computer vision*, 280–296. Springer.
- Lin, X.; Xiang, Y.; Zhang, L.; Yang, X.; Yan, Z.; and Yu, L. 2023. SAMUS: Adapting segment anything model for clinically-friendly and generalizable ultrasound image segmentation. *arXiv preprint arXiv:2309.06824*.
- Liu, R.; Xiao, H.; Wang, Y.; Zhang, M.; Meng, B.; Long, X.; and Liu, J. 2024. Exploring Domain Generalization in Semantic Segmentation for Digital Histopathology: A Comparative Evaluation of Deep Learning Models. In *International Conference on Biomedical Signal and Image Processing*.
- Ma, J.; He, Y.; Li, F.; Han, L.; You, C.; and Wang, B. 2024. Segment anything in medical images. *Nature Communications*, 15(1): 654.
- Mazurowski, M. A.; Dong, H.; Gu, H.; Yang, J.; Konz, N.; and Zhang, Y. 2023. Segment anything model for medical image analysis: an experimental study. *Medical Image Analysis*, 89: 102918.
- MIaMIA. 2022. EBHI-SEG.

- Oktay, O.; Schlemper, J.; Folgoc, L. L.; Lee, M.; Heinrich, M.; Misawa, K.; Mori, K.; McDonagh, S.; Hammerla, N. Y.; Kainz, B.; et al. 2018. Attention u-net: Learning where to look for the pancreas. *arXiv preprint arXiv:1804.03999*.
- Raghu, M.; Unterthiner, T.; Kornblith, S.; Zhang, C.; and Dosovitskiy, A. 2021. Do vision transformers see like convolutional neural networks? *Advances in neural information processing systems*, 34: 12116–12128.
- Riera-Marín, M.; Kleiß, J.-M.; Aubanell, A.; and Antolín, A. 2024. CURVAS dataset.
- Ronneberger, O.; Fischer, P.; and Brox, T. 2015. U-net: Convolutional networks for biomedical image segmentation. In *Medical image computing and computer-assisted intervention—MICCAI 2015: 18th international conference, Munich, Germany, October 5-9, 2015, proceedings, part III 18*, 234–241. Springer.
- Tang, Y.; He, Y.; Nath, V.; Guo, P.; Deng, R.; Yao, T.; Liu, Q.; Cui, C.; Yin, M.; Xu, Z.; et al. 2024. HoloHisto: End-to-end Gigapixel WSI Segmentation with 4K Resolution Sequential Tokenization. *arXiv preprint arXiv:2407.03307*.
- Valanarasu, J. M. J.; Oza, P.; Hacihaliloglu, I.; and Patel, V. M. 2021. Medical transformer: Gated axial-attention for medical image segmentation. In *Medical image computing and computer assisted intervention—MICCAI 2021: 24th international conference, Strasbourg, France, September 27–October 1, 2021, proceedings, part I 24*, 36–46. Springer.
- Wahid, K.; Dede, C.; Naser, M.; and Fuller, C. 2024. Training Dataset for HNTSMRG 2024 Challenge.
- Wang, Y.; Zhang, Y.; Chen, X.; Wang, S.; Qian, D.; Ye, F.; Xu, F.; Zhang, H.; Zhang, Q.; Wu, C.; et al. 2024. STS MICCAI 2023 Challenge: Grand challenge on 2D and 3D semi-supervised tooth segmentation. *arXiv preprint arXiv:2407.13246*.
- Yang, Z.; and Farsiu, S. 2023. Directional connectivity-based segmentation of medical images. In *Proceedings of the IEEE/CVF conference on computer vision and pattern recognition*, 11525–11535.
- Ye, J.; Cheng, J.; Chen, J.; Deng, Z.; Li, T.; Wang, H.; Su, Y.; Huang, Z.; Chen, J.; Jiang, L.; et al. 2023. Sa-med2d-20m dataset: Segment anything in 2d medical imaging with 20 million masks. *arXiv preprint arXiv:2311.11969*.
- Zhang, K.; and Liu, D. 2023. Customized segment anything model for medical image segmentation. *arXiv preprint arXiv:2304.13785*.
- Zhang, Y.; Liu, H.; and Hu, Q. 2021. Transfuse: Fusing transformers and cnns for medical image segmentation. In *Medical image computing and computer assisted intervention—MICCAI 2021: 24th international conference, Strasbourg, France, September 27–October 1, 2021, proceedings, Part I 24*, 14–24. Springer.
- Zhang, Y.; Shen, Z.; and Jiao, R. 2024. Segment anything model for medical image segmentation: Current applications and future directions. *Computers in Biology and Medicine*, 108238.
- Zhou, Z.; Rahman Siddiquee, M. M.; Tajbakhsh, N.; and Liang, J. 2018. Unet++: A nested u-net architecture for medical image segmentation. In *Deep Learning in Medical Image Analysis and Multimodal Learning for Clinical Decision Support: 4th International Workshop, DLMIA 2018, and 8th International Workshop, ML-CDS 2018, Held in Conjunction with MICCAI 2018, Granada, Spain, September 20, 2018, Proceedings 4*, 3–11. Springer.